Bounds on the Hausdorff Dimension of a Renormalisation Map arising from an Excitable Reaction-Diffusion System on a Fractal Lattice

Anthony J. Mulholland[1]

Department of Mathematics, University of Strathclyde, Glasgow, U.K.

Abstract

A renormalisation approach to investigate travelling wave solutions of an excitable reaction-diffusion system on a deterministic fractal structure has recently been derived. The dynamics of a particular class of solutions which are governed by a two dimensional subspace of these renormalisation recursion relationships are discussed in this paper. The bifurcations of this mapping are discussed with reference to the discontinuities which arise at the singularities. The map is chaotic for a bounded region in parameter space and bounds on the Hausdorff dimension of the associated invariant hyperbolic set are calculated.

1. Introduction

There have been a number of mathematical approaches which describe wave propagation in fractal media [1–8]. In particular, a series of papers have been devoted to transport equations with first order reaction schemes in a class of deterministic fractal media [9–19]. In this paper an input/output renormalisation scheme is used to model

[1]Department of Mathematics, University of Strathclyde, Livingstone Tower, 26 Richmond Street, Glasgow G1 1XH, U.K., Tel: ++44 (0)141 548 2971, Fax: ++44 (0)141 548 3345, email: ajm@maths.strath.ac.uk

excitable reaction-diffusion waves in a fractal lattice. The input/output renormalisation approach is restricted to the study of linear field equations [9] and so investigating the dynamics of (nonlinear) excitable reaction-diffusion systems would not normally be possible. However, a piecewise linear model exists for the study of nonlinear reaction-diffusion waves in a Euclidean domain [20]. The behaviour of this model is qualitatively the same as the nonlinear case; both models support travelling waves, are excitable, and exhibit threshold behaviour and wave annihilation. One difference arises in the relationship between the wave speed and the kinetic parameter a. For the cubic nonlinearity the wave speed is finite as $a \to 0^+$, whereas in the piecewise linear case the wave speed becomes unbounded as $a \to 0^+$. Numerical studies have shown that the Sierpinski gasket pre-fractal lattices can support travelling waves for this system [21, 22]. The waves are step-like in nature with a steep front connecting the excited and quiescent states. The linear field equations are solved in each of the two regions on either side of the transition layer and then interface conditions are imposed to connect these two solutions. Section 2 provides a brief derivation of the renormalisation scheme which has been used to study the existence and stability of travelling waves on a fractal lattice [21, 22]. In Section 3 a two dimensional subspace of the renormalisation recursion relationships is examined. The phase space trajectories of these coupled maps form a family of hyperbolae. By an appropriate parameterisation, this leads to transformations which decouple the maps and provide analytic expressions for their evolution. The maps are chaotic and bounds on the fractal dimension of the associated invariant set are calculated.

2. Renormalisation of an Excitable Reaction-Diffusion System in a Fractal Lattice.

The following excitable reaction-diffusion (RD) system will be studied in this paper. It has been used extensively to provide analytical expressions for travelling waves in Euclidean media. The reaction term is $f(v) = v - H(v - a)$, $0 \leq a \leq 0.5$ (H denotes the Heaviside step function), g and b are reaction coefficients [20], and the model is

$$\begin{aligned} \frac{\partial v}{\partial t} &= \epsilon D \nabla^2 v - \frac{g}{\epsilon}(f(v) + w) \\ \frac{\partial w}{\partial t} &= \frac{b}{\epsilon} v, \quad b \geq 0 \end{aligned} \tag{1}$$

subject to the boundary conditions $|v|, |w| \to 0$ as $|z| \equiv |x+ct| \to 0$. The small parameter $\epsilon \ll 1$ is used to balance the levels of reaction and diffusion, which ultimately dictates the propagation characteristics of the wave. It has recently been shown that a renormalisation approach can be used to study this model on a fractal lattice [21,22] and for completeness an overview of this methodology is presented below. The deterministic fractal supports are defined recursively to form a family of graphs

$$\Psi^{(n+1)} = \Im[\Psi^{(n)}]. \tag{2}$$

Each graph consists of v copies of itself at level n to form its equivalent at level $n+1$. The adjacency matrix $H^{(n)}$ describes the connectivity properties of the graph with its $(i,j)^{th}$ element giving the number of edges connecting site i to site j. The family of graphs considered in this paper has a number of nodes $N_n = 3^n$ and the total number of edges emanating from a given node is a constant, $p = 3$. The recursive nature of these graphs can be expressed as

$$H^{(n+1)} = \overline{H}^{(n)} + V^{(n)} \tag{3}$$

where $\overline{H}^{(n)}$ is a block diagonal matrix, whose blocks are equal to $H^{(n)}$, and $V^{(n)}$ is the connection matrix. $V^{(n)}$ is a sparse matrix, containing a constant number of nonzero elements. It represents the connection of the output nodes between the different subgraph blocks, each of which is a copy of $\Psi^{(n)}$. These are connected at the n^{th} recursion step in order to form $\Psi^{(n+1)}$. Therefore this study is restricted to the case of a finitely ramified fractal.

The Sierpinski Gasket lattice $SG(p)$ is the lattice counterpart of the Sierpinski gasket SG. The procedure starts from the SG of order 2 which consists of three solid triangles. Nodes at the centre of each of these triangles are connected by an edge to get an equilateral

triangle which is the $SG(3)$ lattice at generation level $n = 1$. This process is then repeated for each generation of the SG (see Figure 1).

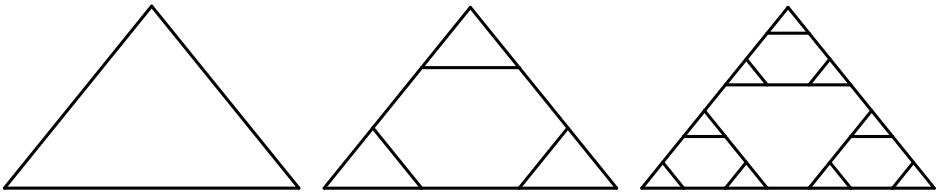

E_1 E_2 E_3

Figure 1: The pre-fractals E_1, E_2 and E_3 for the $SG(3)$ lattice.

For each node of the lattice Fick's law is applied with regard to the nearest neighbour nodes. Coupling this with mass conservation, and comparing with the diffusion equation, gives the discrete Laplacian operator, for level n [10]

$$\nabla^2 = (H^{(n)} - pI)/\triangle x^2 = A^{(n)}/\triangle x^2. \tag{4}$$

Note that $\triangle x = l/(2^n - 1)$ decreases to zero as n increases since the characteristic size of the structure l remains constant. The co-ordination number is p at each internal node in the structure and $p - 1$ at the input/ output nodes, where $p = \sum_{j=1}^{N_n} H_{ij}$. A travelling wave can be instigated on the SG(3) lattice by exciting a set of nodes on an outer edge (opposite the bottom left corner $x = 0$). A numerical demonstration of the ability of the SG(3) graph to support such waves has been reported in [21]. The wave profile is step-like with each field variable monotonically decreasing from the excited steady-state, through a steep transition region and into the unexcited (trivial) steady-state. Equation (1) can be put into a travelling coordinate frame $z = x + ct$, where c is the velocity of the wave front and x is the length of the shortest path on the SG(3) lattice from the (bottom left corner) output node of the lattice. Combining the resulting equations gives

$$c\frac{d^2 v_i^{(n)}}{dz^2} = \epsilon D\frac{d\nabla^2 v_i^{(n)}}{dz} - \frac{g}{\epsilon}\frac{df(v_i^{(n)})}{dz} - \frac{gb}{\epsilon^2 c}v_i^{(n)} \quad , \tag{5}$$

where

$$\frac{df(v_i)}{dz} = \begin{cases} \dfrac{v_i - v_j + 1}{\triangle z} & \text{if } v_j > a \text{ and } v_i < a \\ \dfrac{v_i - v_j - 1}{\triangle z} & \text{if } v_i > a \text{ and } v_j < a \\ \dfrac{v_i - v_j}{\triangle z} & \text{Otherwise} \end{cases}, \tag{6}$$

and $v_i^{(n)}$ is the level of the state variable v at node i, at generation level n. Travelling wave solutions of (5) will be of the form of a step-like wave with $v = v^-$ for $z \to -\infty$, $v = v^+$ for $z \to +\infty$ and $v^- < v^+$. The transition layer is located at $v = a$ ($v^- < a < v^+$) and equation (6) details the various forms of the discretised, nonlinear reaction term at this interface and in each of the adjacent linear regions. Each of the operators in (5) is written in matrix form by discretising the independent variable z (see [21] for full details). Each of these matrices is formulated at generation level $n = 2$ with number of nodes $N_n = 3^n = 9$. Three fictitious nodes are introduced; A, B and C (see Figure 2). These correspond to the input/output nodes which by enforcing the boundary conditions, close the system of equations. For order n the input/output nodes are numbered 1, m and N_n respectively, where $m = \frac{N_n+1}{2}$, and the value of v at each fictitious node is denoted by v_A, v_B and v_C. Each of the terms in equation (5) is then expressed as a discrete operator using the same methodology used to discretise the Laplacian [21], to give

$$\begin{aligned}(\frac{c}{\triangle z^2}R^{(n)} - \frac{\epsilon D}{\triangle z^3}M^{(n)} - \frac{g}{\epsilon \triangle z}K^{(n)} + \frac{gb}{\epsilon^2 c}I^{(n)})\underline{v} = (\frac{-c}{\triangle z^2} - \frac{\epsilon D}{\triangle z^3} + \frac{g}{\epsilon \triangle z})v_A\underline{e}_1 \\ + (\frac{-c}{\triangle z^2} + \frac{\epsilon D}{\triangle z^3})(v_B\underline{e}_m + v_C\underline{e}_{N_n}).\end{aligned} \tag{7}$$

where $\underline{e}_j$ are basis vectors. The reaction-diffusion waves are not scale invariant and have a characteristic length scale given by the front width L. The small parameter ϵ can be expressed in terms of this length scale by setting $\epsilon = \triangle z/L$. Equation (7) can then be non-dimensionalised in terms of the Peclet number $Pe = \dfrac{cL}{D}$ and the Thiele modulus, $\phi = L\sqrt{\dfrac{g}{D}}$, to give [21]

$$(\frac{Pe^2}{\phi^2}R^{(n)} - \frac{Pe}{\phi^2}M^{(n)} + PeK^{(n)} + \phi^2 I^{(n)})\underline{v} = (\frac{-Pe^2}{\phi^2} - \frac{Pe}{\phi^2} + Pe)v_A\underline{e}_1$$

$$+(\frac{-Pe^2}{\phi^2}+\frac{Pe}{\phi^2})(v_B\underline{e}_m+v_C\underline{e}_{N_n}), \tag{8}$$

where for simplicity g has been set equal to b. The right hand side can be expressed in terms of a transfer matrix $G^{(n)}$ to give

$$G^{(n)}\underline{v}=k_1v_A\underline{e}_1+k_2(v_B\underline{e}_m+v_C\underline{e}_{N_n}), \tag{9}$$

where $k_1=\dfrac{-Pe^2}{\phi^2}-\dfrac{Pe}{\xi\phi^2}+\xi Pe$ and $k_2=\dfrac{-Pe^2}{\phi^2}+\dfrac{Pe}{\xi\phi^2}$. To solve this set of linear equations in $\underline{v}$ the resolvent $F^{(n)}=(G^{(n)})^{-1}$ must be calculated. Inverting G directly is computationally prohibitive and, in addition, the case $n\to\infty$ is of interest since it corresponds to the true fractal support [22]. By writing $G^{(n+1)}=\overline{G}^{(n)}+T^{(n)}$, where $T^{(n)}$ is a sparse matrix, it is possible to derive the following renormalisation recursion relationship

$$F^{(n+1)}=\overline{F}^{(n)}-\overline{F}^{(n)}T^{(n)}F^{(n+1)}. \tag{10}$$

This can then be used to calculate the pivotal elements of $F^{(n)}$ at each generation level. The elements of $T^{(n)}_{hk}$ represent the edges which connect the three copies of $F^{(n)}$ to generate $F^{(n+1)}$. Therefore it is a very sparse matrix and coupling this with the $SG(3)$ symmetry ensures a substantial reduction in the number of equations to be solved. To utilise the recursive relationship (10), the $SG(3)$ at level $n=2$ is considered as an initial structure and related to the same structure at level $n=3$ (see Figure 2). The resolvent $F^{(2)}$ is then calculated by directly inverting $G^{(2)}$. It transpires that the following set of fourteen recursion relationships can be used to calculate the pivotal elements of the F at any level [21]

$$F^{(n+1)}_{1,1}=F^{(n)}_{1,1}+2k_2F^{(n)}_{1,5}F^{(n+1)}_{10,1}\ , \tag{11}$$

$$F^{(n+1)}_{10,1}=k_1F^{(n)}_{1,1}F^{(n+1)}_{5,1}+k_2F^{(n)}_{1,5}F^{(n+1)}_{18,1}\ , \tag{12}$$

$$F^{(n+1)}_{18,1}=k_1F^{(n)}_{5,1}F^{(n+1)}_{5,1}+k_2F^{(n)}_{5,5}F^{(n+1)}_{18,1}\ , \tag{13}$$

$$F^{(n+1)}_{5,1}=F^{(n)}_{5,1}+k_2(F^{(n)}_{5,5}+F^{(n)}_{5,9})F^{(n+1)}_{10,1}\ , \tag{14}$$

$$F^{(n+1)}_{14,1}=k_1F^{(n)}_{5,1}F^{(n+1)}_{5,1}+k_2F^{(n)}_{5,9}F^{(n+1)}_{18,1}\ , \tag{15}$$

$$F_{1,14}^{(n+1)} = k_2 F_{1,5}^{(n)} F_{10,14}^{(n+1)} + k_2 F_{1,5}^{(n)} F_{10,27}^{(n+1)} \ , \tag{16}$$

$$F_{10,14}^{(n+1)} = F_{1,5}^{(n)} + k_1 F_{1,1}^{(n)} F_{5,14}^{(n+1)} + k_2 F_{1,5}^{(n)} F_{18,27}^{(n+1)} \ , \tag{17}$$

$$F_{10,27}^{(n+1)} = k_1 F_{1,1}^{(n)} F_{5,27}^{(n+1)} + k_2 F_{1,5}^{(n)} F_{18,14}^{(n+1)} \ , \tag{18}$$

$$F_{5,14}^{(n+1)} = k_2 F_{5,5}^{(n)} F_{10,14}^{(n+1)} + k_2 F_{5,9}^{(n)} F_{10,27}^{(n+1)} \ , \tag{19}$$

$$F_{18,27}^{(n+1)} = k_1 F_{5,1}^{(n)} F_{5,27}^{(n+1)} + k_2 F_{5,5}^{(n)} F_{18,14}^{(n+1)} \ , \tag{20}$$

$$F_{5,27}^{(n+1)} = k_2 F_{5,5}^{(n)} F_{10,27}^{(n+1)} + k_2 F_{5,9}^{(n)} F_{10,14}^{(n+1)} \ , \tag{21}$$

$$F_{18,14}^{(n+1)} = F_{5,9}^{(n)} + k_1 F_{5,1}^{(n)} F_{5,14}^{(n+1)} + k_2 F_{5,5}^{(n)} F_{18,27}^{(n+1)} \ , \tag{22}$$

$$F_{14,14}^{(n+1)} = F_{5,5}^{(n)} + k_1 F_{5,1}^{(n)} F_{5,14}^{(n+1)} + k_2 F_{5,9}^{(n)} F_{18,27}^{(n+1)} \ , \tag{23}$$

$$F_{14,27}^{(n+1)} = k_1 F_{5,1}^{(n)} F_{5,27}^{(n+1)} + k_2 F_{5,9}^{(n)} F_{18,14}^{(n+1)} \ . \tag{24}$$

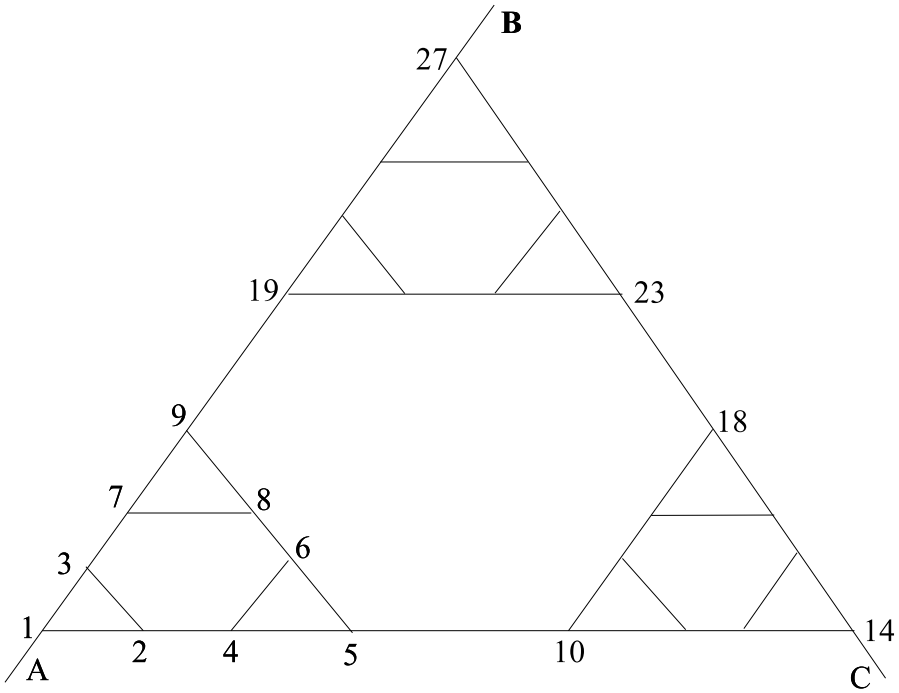

Figure 2: The node labelling for the Sierpinski gasket lattice at level $n = 3$.

This methodology has been used to investigate the existence and stability of travelling waves for both finite generation level (pre-fractal) and infinite generation level (fractal) supports [21,22]. Note that the elements at level $n+1$ only depend on five pivotal elements at level n, namely $u = F_{1,1}^{(n)}$, $v = F_{1,5}^{(n)}$, $w = F_{5,1}^{(n)}$,$y = F_{5,5}^{(n)}$ and $x = F_{5,9}^{(n)}$ (this notation

is introduced to simplify the presentation). By scaling the variables $F_{5,1}^{(n)}$, $F_{1,1}^{(n)}$, $F_{10,1}^{(n+1)}$, $F_{18,1}^{(n+1)}$, and $F_{5,1}^{(n+1)}$ by k_1 and the remaining variables by k_2, and denoting the elements of F at generation $n+1$ by capital letters, these fourteen equations can be reduced to the four pivotal relationships

$$X = \frac{x^2 - (v^2 - u\,x)^2\ (x^2 - y^2) - x\ \left(2\,u\,x\,y - v^2\ \left(1 - (x-y)^2 + 2\,y\right)\right)}{(1 - y - v^2\ (x+y) - u\ (1-y)\ (x+y))\ (1 + y + (x-y)\ (u - v^2 + u\,y))} \tag{25}$$

$$Y = X + y + \frac{v^2\ (2\,x^2 - x + y - 3\,x\,y + y^2) - x^2\ (1 + u\ (x-y))}{1 + y + u\ (x-y)\ (1+y) + v^2\ (y-x)} \tag{26}$$

$$U = \frac{2\,v^4 + u^2\ (y-1)\ (x+y) + u\ (1 - y + v^2\ (2 - x - 3\,y))}{1 - y - v^2\ (x+y) + u\ (y-1)\ (x+y)} \tag{27}$$

$$V = \frac{v^2\ (1 + x - y)}{1 - y - v^2\ (x+y) + u\ (y-1)\ (x+y)} \tag{28}$$

where the isotropic condition $w = v$ is set (the system is invariant under the interchange of w and v).

3. A Two Dimensional Subspace of the Renormalisation Recursion Relationships.

Numerical iteration of equations (25) to (28)indicate that for certain initial conditions the pivotal elements in the resolvent tend to a subspace where $v = 0$, u is a constant, and where x and y behave randomly as the generation level n increases. Setting $v = 0$ and $u =$ constant in equations (25) to (28), the remaining pivotal elements are defined by the mapping $\phi : (x, y) \to (X, Y)$, defined by

$$Y = y(1 + \frac{x^2}{1 - y^2})\ , \tag{29}$$

$$X = \frac{x^2}{1 - y^2}\ . \tag{30}$$

This planar mapping is the same as that derived in [19] for the case of the Schrodinger equation on a linear chain lattice.

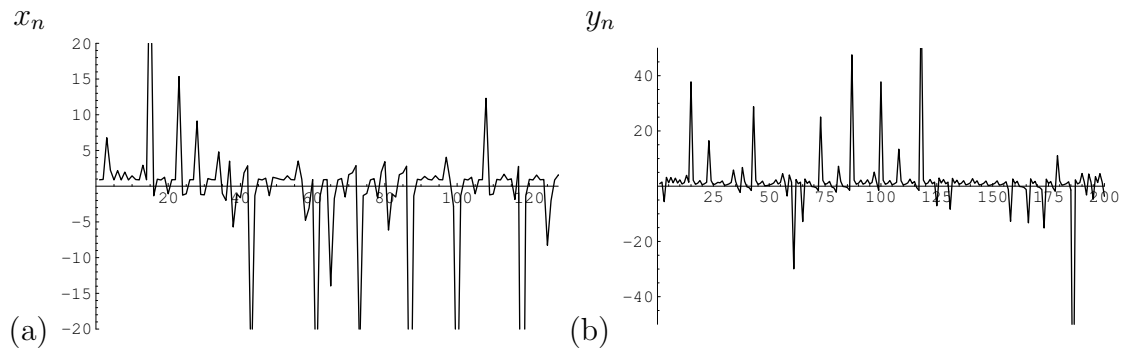

Figure 3: (a) x_n versus the iteration number n, (b) y_n versus the iteration number n.

Although the iteration of this mapping appears to be random for certain initial conditions (see Figure 3), with no obvious correlation between successive terms, a phase space plot of y versus x shows a trajectory in the shape of a hyperbola (see Figure 4). By varying the initial conditions, a family of hyperbolic trajectories can be found; if the initial conditions lie within the set shown in Figure 5. Initial conditions outside this domain iterate to steady state solutions on the y-axis. These solutions correspond to waves propagating on the true fractal (infinite number of generation levels) and have been discussed in [22].

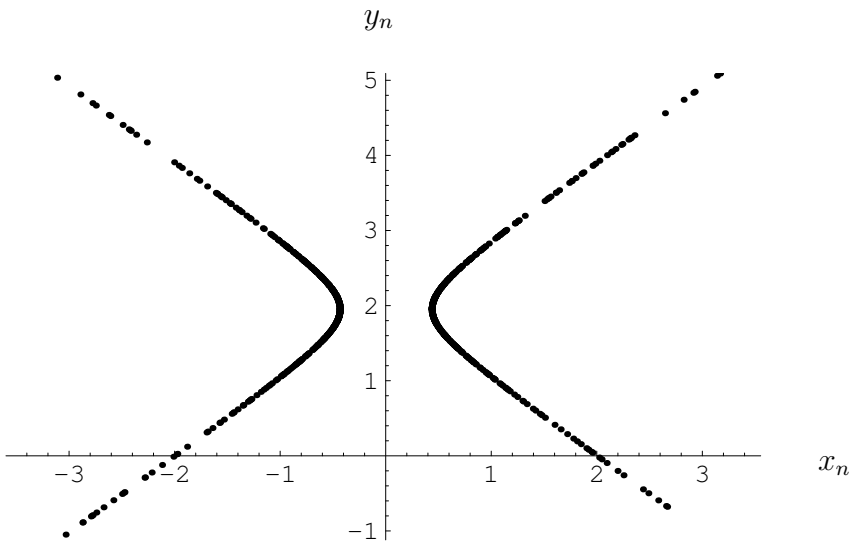

Figure 4: A phase space trajectory of y_n versus x_n.

This can be shown by perturbing the pivotal elements by $\underline{q}^{(n)} = (q_x^{(n)}, q_y^{(n)}, q_u^{(n)}, q_v^{(n)})$, where $|q_i^{(n)}| \ll 1$ and iterating the pivotal recursions $\underline{X} = \underline{\zeta}(\underline{x})$ numerically. This shows that u tends to a constant value, which is approximately its initial value translated by the

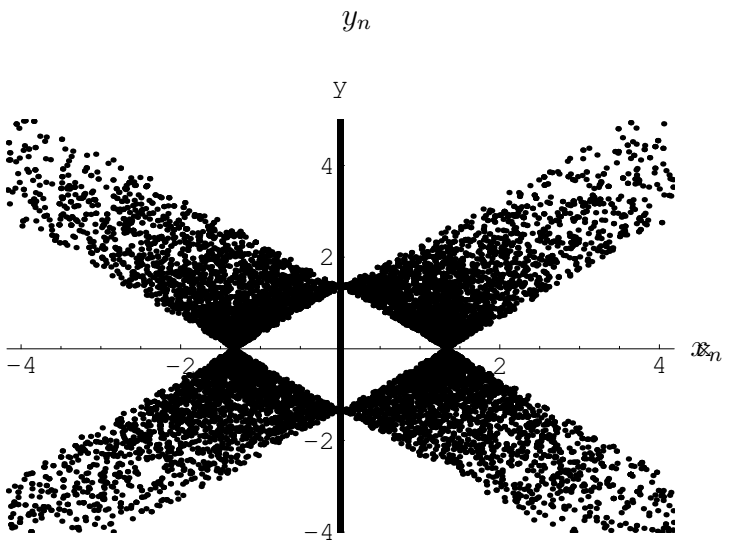

Figure 5: The domain of attraction for chaotic orbits in (x_n,y_n).

perturbation $q_u^{(0)}$. It also shows that v tends to zero whereas x and y behave chaotically. Using a Taylor series expansion gives

$$\underline{Q} = \underline{\zeta}'(\underline{x})\underline{q} + \frac{1}{2}\underline{\zeta}''(\underline{x})\underline{q}^2 + O(\underline{q}^3) \tag{31}$$

Now the subspace is stable if $|\underline{Q}| < |\underline{q}|$. To order $\underline{q}^2$, $|q_v^{(n+2)}| < |q_v^{(n)}|$ if $q_v^{(0)}$ is small enough to guarantee

$$\left(\frac{1-Y+X}{(1-Y)(1-U(Y+X)}\right)\left(\frac{1-y+x}{(1-y)(1-u(y+x)}\right)^2 (q_v^{(0)})^3 < 1.$$

A similar analysis shows that $q_u^{(n)} \to q_u^{(0)}$ as $n \to \infty$, as predicted by the numerical simulation.

3.1 Bounds on the Hausdorff dimension of the Invariant Hyperbolic Set.

Using a group theoretic approach it is possible to derive a transformation to decouple the mappings (29) and (30) [6,7,18] (see Appendix). Analysis of equations (25) to (28) using a Lie group approach [23,24] may lead to a similar decoupling and this is currently being investigated. The transformation $\psi : (a_n, t_n) \to (x_n, y_n)$ defined by

$$x_n = \frac{(1-a)t}{2} + \frac{1+a}{2t} \tag{32}$$

$$y_n = \frac{1+a}{2t} - \frac{(1-a)t}{2} - a, \tag{33}$$

also decouples the mappings (29) and (30). The inverse transformation $\psi^{-1} : (x_n, y_n) \rightarrow (a_n, t_n)$ is

$$a_n = \frac{k^2x_n^2 - k^2y_n^2 - 1}{2ky_n} \tag{34}$$

$$t_n = \frac{kx_n - ky_n + 1}{kx_n + ky_n + 1}\ , \tag{35}$$

and the composition $\Phi = \psi^{-1}\phi\psi$, maps (a_n, t_n) into (a_{n+1}, t_{n+1}) via

$$a_{n+1} = a_n \tag{36}$$

$$t_{n+1} = \frac{(1-a_n)t_n^2 + (2a_n+2)t_n - (1+a_n)}{(a_n-1)t_n^2 - (2a_n-2)t_n + (1+a_n)}\ . \tag{37}$$

Here a_0 sets the particular member of the hyperbola family and t_0 parameterises it. This gives a parameterised family of functions $f_a(t)$ where

$$t_{n+1} = f_a(t_n) = \frac{(1-a)t_n^2 + (2a+2)t_n - (1+a)}{(a-1)t_n^2 - (2a-2)t_n + (1+a)}\ . \tag{38}$$

The map $f_a(t_n)$ has three fixed points $t^* = \{1, -\frac{\sqrt{a^2-1}}{1-a}, \frac{\sqrt{a^2-1}}{1-a}\}$. The nature of these fixed points for all cases of the parameter a can be examined using the derivative $f'_a(t_n)$ at each point ([25], p.24). It transpires that,

(i) $t_1^* = 1$ is a repelling fixed point for all values of a (see Figure 6).

(ii) $t_2^* = -\sqrt{\frac{a+1}{a-1}}$ and $t_3^* = \sqrt{\frac{a+1}{a-1}}$ are attracting fixed points for $|a| > 1$ (see Figures 6(b) and (e)).

Numerical evidence suggests that for $a = -1$, the origin is a global attracting fixed point, when $a = 1$ all orbits tend to infinity, and for $|a| < 1$ the map $f_a(t_n)$ behaves chaotically (see Figure 7).

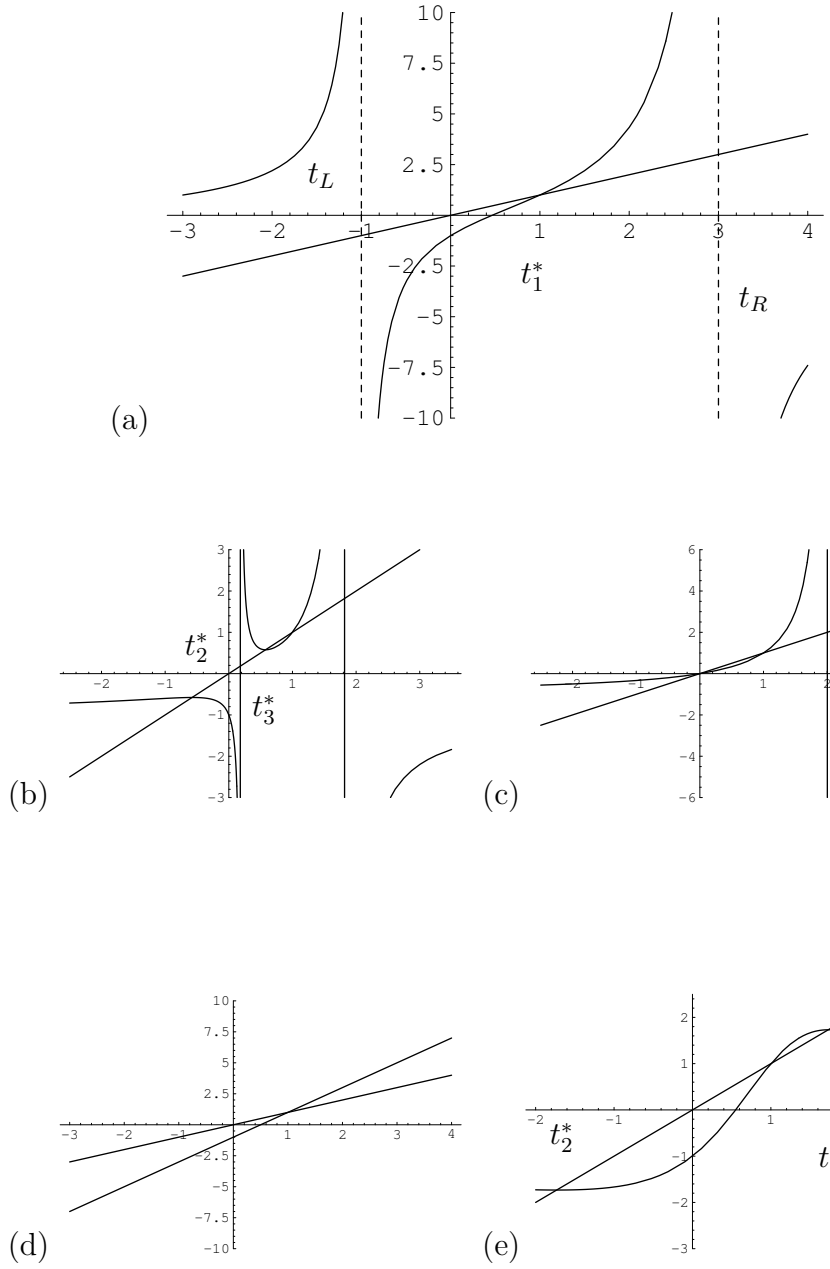

Figure 6: The function $f_a(t_n)$ versus t_n for different values of a; (a) $|a| < 1$, (b) $a < -1$, (c) $a = -1$, (d) $a = 1$ and (e) $a > 1$. The vertical asymptotes are t_L, $t_R = 1 \mp \sqrt{\frac{2}{1-a}}$, and f_a cuts the t-axis at t_A, $t_B = \frac{(a+1)\mp\sqrt{2(1+a)}}{a-1}$.

For $a < -1$ there are two attracting fixed points t_2^* and t_3^*, separated by the singularity at t_L (see Figure 8(b)). These approach one another as the parameter a increases, and then coalesce to form a globally attracting fixed point at the origin when $a = -1$ (see Figure 6(c)). As a is increased further a singularity appears at $1 - \sqrt{\frac{2}{1-a}}$, the attracting

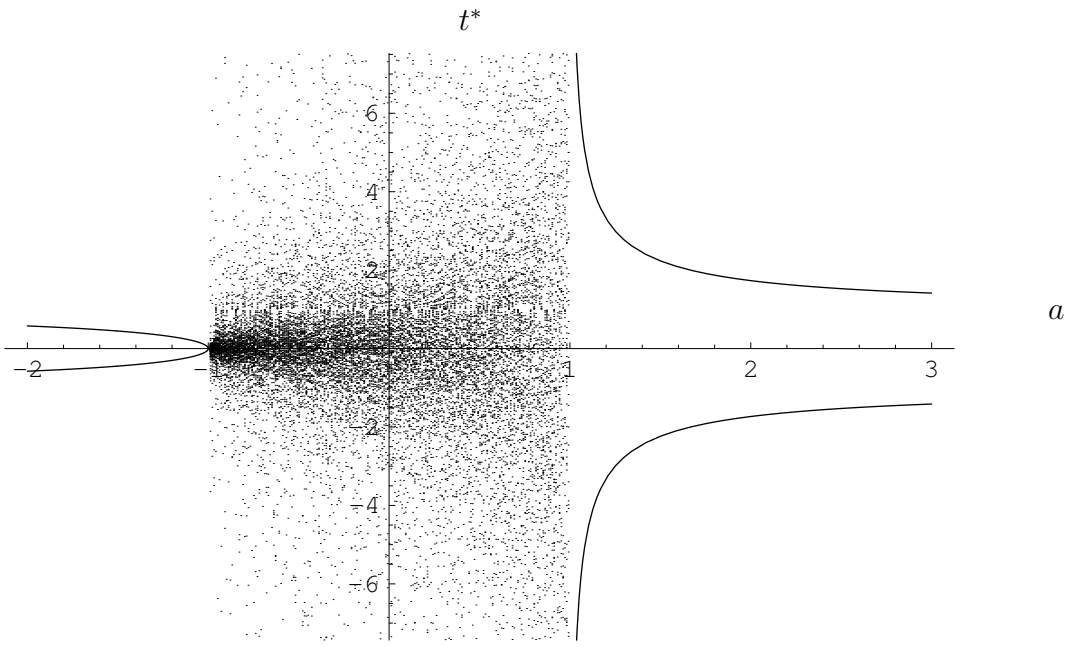

Figure 7: The bifurcation diagram of $f_a(t_n)$.

fixed point disappears and this leaves a single repelling fixed point at $t_1^* = 1$ (see Figure 6(a)). It is observed that at this point a bifurcation to chaotic behaviour occurs (see Figure 7) without any period doubling cascade. Although this has the hallmarks of a saddle-node bifurcation, ([26], p.60) two fixed points coalescing and eventually vanishing, this does not occur through a tangent of the graph of $f_a(t_n)$ but rather through the birth of a singularity in the function. Also note that the fixed points satisfy $|f_a'(t_j^*)| \neq 1$ and are therefore hyperbolic ([27], p.24). Increasing a still further to $a = 1$, both the singularities disappear to leave a linear function with the sole repelling fixed point at $t_1^* = 1$ remaining. As a increases beyond 1, the two attracting fixed points t_2^* and t_3^* reappear. Denote the *stable set* of a periodic point p of f_a by $W^s(p)$. This is the set of all points q in the domain of f_a where $\lim_{n\to\infty} f_a^n(q) = p$. So for $a < -1$, $W^s(t_3^*) = (\frac{a+1}{a-1}, 1)$ and $W^s(t_2^*) = (-\infty, \frac{a+1}{a-1}) \cup (1, \infty)$, and for $a > 1$, $W^s(t_2^*) = (-\infty, 1) \cup (\frac{a+1}{a-1}, \infty)$ and $W^s(t_3^*) = (1, \frac{a+1}{a-1})$. For $|a| < 1$ the *local unstable set* $(W_{loc}^u(t_1^*))$ of the repelling fixed point t_1^* is (t_L, t_R) since $f_a'(t_n) > 1$, for all $t_n \in (t_L, t_R)$. Also note that $f_a'(t_n) = 0$ only when $t_n = \{t_2^*, t_3^*\}$ and so $f_a'(t_n) \neq 0$, for all t_n if $|a| < 1$. A homoclinic orbit $\{q_i\}$, $i = 0, 1, \ldots$ can be found by solving $f_a^i(q_i) = t_1^*$ for each i, where $q_i \in W_{loc}^u(t_1^*)$ for $|a| < 1$. Solving

$f_a^2(q_0) = t_1^*$ for $q_0 \in W^u_{loc}(t_1^*)$ gives four roots $q_0 = \{1, \frac{1+a}{a-1}, \frac{(a^2-1)-\sqrt{1-a^2}}{a^2-a}, \frac{(a^2-1)+\sqrt{1-a^2}}{a^2-a}\}$. However it can be shown that only $q_0 = \frac{(a^2-1)+\sqrt{1-a^2}}{a^2-a} \in W^u_{loc}(t_1^*)$.

For example, if $a = 0.5$ then $q_0 = -0.464102$ and working backwards one iteration, that is solving $f_a(q_1) = q_0$, gives $q_1 = 0.228029$. Continuing this process generates the homoclinic orbit $\{q_i\}$ and, since for $|a| < 1$ $f_a'(q_i) \neq 0$, the orbit must be nondegenerate. It transpires that f_a^4 is topologically conjugate to the shift map [26]. This particular value of a is used below to demonstrate this. Let $V = [q_0 - 0.1, q_0 + 0.05] = [-0.564102, -0.414102]$ be a neighbourhood of q_0 where $|(f_a^2)'(t)| > \epsilon > 0$, for all $t \in V$. Let $j \geq 1$, $j \in \mathbb{N}$, be such that $\delta^j \epsilon > 1$, that is $j > \dfrac{\log \frac{1}{\epsilon}}{\log \delta}$. Take $\delta = 1.8$ and $\epsilon = j = 1$, so that, $f_a^3(V) = f_a^{n+j}(V) = [0.172366, 1.58337]$ satisfies $f_a^3(V) \cap V = \emptyset$. Now $f_a^{n+j+1}(V) = [-0.584037, 2.46121] = W$, say, and $|(f_a^{n+j+1})'(t)| > 1$, for all $t \in V$. Now let $V' = [t_1^* - 0.11898385, t_1^* + 0.06365] = [0.881016, 1.06365] \subset W$ be a neighbourhood of t_1^* such that,

1. $f_a^{n+j+1}(V') = f_a^4(V')$ is one-to-one on V' and $f_a^4(V') = W$ (see Figure 8).
2. $|(f_a^{n+j+1})'(t)| > 1$, for all $t = V'$ (see Figure 8).
3. $f_a^{n+j+1}(V') \supset V$.
4. $V \cap V' = \emptyset$, and $f_a^{n+j+1}(V')$ covers V'.

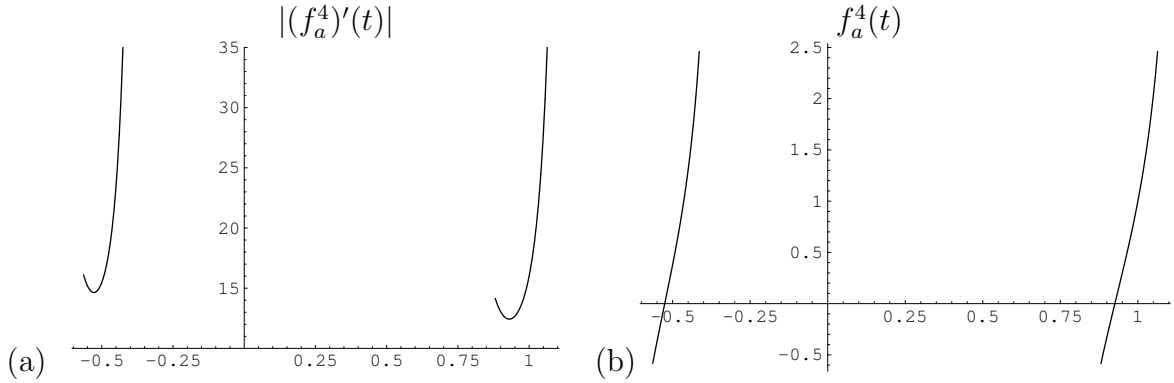

Figure 8: (a) $|(f_a^4)'(t)|$ versus t and (b) $f_a^4(t)$ versus t, where $t \in V \cup V'$ and $a = 0.5$.

Let $A_0 = W/(V \cup V')$ then since $|(f_a^4)'(t)| > 1$, for all $t \in W$ then points in A_0 iterate out of W under f_a^4. Similarly there exists a set A_1 such that $f_a^4(A_1) = A_0$. A_1 consists of two parts, one in V and one in V', which iterate out of W under $(f_a^4)^2$. Continuing in this manner, the set $\Lambda = W/\left(\cup_{n=0}^{\infty} A_n\right)$, can be shown to be a Cantor set, and is a repelling, hyperbolic invariant set for f_a^4 [27].

Let the sequence $S(t) = s_0 s_1 s_2 \ldots$ where

$$s_j = \begin{cases} 0 & f_a^{4j}(t) \in V \\ 1 & f_a^{4j}(t) \in V' \end{cases},$$

be the *itinerary* of t. The mapping $S : \Lambda \to \Sigma_2$ can be shown to be a homeomorphism and it also can be shown that $S \circ f_a^4 = \sigma \circ S$ so that f_a^4 and the shift map σ are topologically conjugate. Having established this conjugacy it is now a straightforward matter to demonstrate that the map f_a^4 has dense orbits, its periodic points are dense, and it is sensitive to initial conditions. Denote the points of Λ by $\{t_{i_1,i_2,\ldots},\ i_j = 0, 1\}$, and let $g_0 : W \to V$ and $g_1 : W \to V'$ be the inverse of f_a^4 restricted to the closed intervals V and V' respectively, where $t_{i_1,i_2,\ldots} = g_{i_1}(t_{i_2,i_3,\ldots})$ and $f_a^4(t_{i_1,i_2,\ldots}) = t_{i_2,i_3,\ldots}$. By the Mean Value Theorem and, since $|(f_a^4)'(t)| > 1$ for all $t \in W$, $g_{0,1}$ are contractions on W and in fact $g_0'(x) \in [0.0218842, 0.0682758]$ and $g_1'(x) \in [0.0285076, 0.0804466]$, for all $t \in W$. So there must be a unique non-empty compact subset Λ of W satisfying $\Lambda = g_0(\Lambda) \cup g_1(\Lambda)$ [28]. A lower bound for $\dim_H \Lambda$ is then given by the solution to $0.0218842^s + 0.0285076^s = 1$, and an upper bound by $0.0682758^s + 0.0804466^s = 1$ which gives $0.187939 \leq \dim_H \Lambda \leq 0.266463$. Tighter bounds on $\dim_H \Lambda$ can be found by noting that Λ is also invariant under the four contractions given by $g_i \circ g_j$, $i, j = 0, 1$, so that $0.213448 \leq \dim_H \Lambda \leq 0.258045$.

5 Conclusions.

The input/output renormalisation method is one approach to studying the dynamics of wave processes in fractal graphs. However it is restricted to the study of linear field equations. In this paper a piecewise linear caricature of a nonlinear reaction-diffusion system is used to study the propagation of excitable waves on a Sierpinski gasket lattice. The behaviour of the piecewise linear model is qualitatively the same as the nonlinear case in Euclidean domains; both models support travelling waves, are excitable, and exhibit threshold behaviour and wave annihilation. The renormalisation scheme is applied on either side of the sharp transition layer and then interface conditions are imposed. Previous work has reported on the existence of travelling waves using this technique.

In this paper the dynamics of one class of solutions to the system of renormalisation recursion relationships is studied. When the recursion relationships are iterated they invariably converge to an equilibrium state as the generation level increases. However, for certain parameter regimes, the elements of the Green transfer matrix behave in a chaotic manner from one generation level to the next. Although the recursion equations are complicated one can find some subclasses of solutions. This paper examines in detail one such subclass which is described by a planar coupled nonlinear map in terms of two of the pivotal elements. It transpires that this planar mapping is identical to that derived for the case of the Schrodinger equation on a linear chain lattice. The map undergoes a bifurcation to chaos and this is shown analytically by finding a homeomorphism to the shift map. There is an associated hyperbolic invariant set of Cantor type and bounds on its Hausdorff dimension are calculated in a particular case.

References

[1] Kigami J., (1993) *Harmonic Calculus on P.C.F. Self-similar Sets,* Trans. AMS, 335(2), pp721-755.

[2] Lapidus M. L., (1994) *The Vibrations of Fractal Drums and Waves in Fractal Media,* in, Fractals in the Natural and Applied Sciences (A-41), ed., M.M. Novak, Elsevier Science B.V., North-Holland, pp255-260.

[3] Yamaguti M., Hata M. and Kigami J., (1997) *Mathematics of Fractals,* American Mathematical Society, Translations of Mathematical Monographs, Rhode Island, Vol. 167, ISBN 0-8218-0537-1.

[4] Schwalm W.A. and Schwalm M.K., (1988) *Extension Theory for Lattice Green Functions,* Phys. Rev. B, 37(16), pp9525-9542.

[5] Schwalm W.A. and Schwalm M.K., (1989) *Electronic Properties of Fractal-Glass Models,* Phys. Rev. B, 39(17), pp12872-12882.

[6] Schwalm W.A. and Schwalm M.K., (1992) *Closed Formulae for Green Functions on Fractal Lattices,* Physica A, 185, pp195-201.

[7] Schwalm W.A. and Schwalm M.K., (1993) *Explicit Orbits for Renormalisation Maps for Green Functions on Fractal Lattices,* Phys. Rev. B, 47(13), pp7847-7858.

[8] Falconer K. and Hu, J.,(2001) *Nonlinear Diffusion Equations on Unbounded Fractal Domains*,J Math Anal App, 256, pp606-624.

[9] Giona M., (1992) *First-order Reaction-Diffusion Kinetics in Complex Fractal Media*, Chem. Eng. Sci., 47(6), pp1503-1515.

[10] Giona M., (1996) *Transport Phenomena in Fractal and Heterogeneous Media: Input/Output Renormalisation and Exact Results.* Chaos, Solitons and Fractals, 7(9), pp1371-1396.

[11] Giona M., (1997) *Chemical Engineering, Fractal and Disordered System Theory: Perspectives, Applications and Future Developments*, Fractals, 5(3), pp333-354.

[12] Giona M., Schwalm W.A., Adrover A. and Schwalm M.K., (1996a) *Analysis of Linear Transport Phenomena on Fractals*, Elsevier, the Chemical Engineering Journal, 64, pp45-61.

[13] Giona M., Schwalm W.A., Schwalm M.K. and Adrover A., (1996b) *Exact Solution of Linear Transport Equations in Fractal Media - I. Renormalisation Analysis and General Theory*, Chem Eng Sci, 51(20), pp4717-4729.

[14] Giona M., Schwalm W.A., Schwalm M.K. and Adrover A., (1996c) *Exact Solution of Linear Transport Equations in Fractal Media- II, Diffusion and Convection*, Chem. Eng. Sci., 51(20), pp4731-4744.

[15] Giona M., Adrover A, Schwalm W.A. and Schwalm M.K., (1996d) *Exact Solution of Linear Transport Equations in Fractal Media- III: Adsorption and Chemical Reaction,* Chem. Eng. Sci., 51(22), pp5065-5076.

[16] Giona M., Adrover A, Schwalm W.A. and Schwalm M.K., (1997) *Solution of Transport Schemes on Fractals by Means of Green Function Renormalisation-Application to Integral Quantities,* Fractals, 5(3), pp473-491.

[17] Giona M. and Adrover A., (1996) *Closed-form Solution for the Reconstruction Problem in Porous Media*, AIChE J, 42(5), pp1407-1415.

[18] Schwalm W.A., Reese C.C., Schwalm M.K. and Wagner C.J., (1994) *Conic Pencils and Renormalisation Dynamics,* Phys. Letts. A, 193, pp238-244.

[19] Schwalm M.K., Giona M., Schwalm W.A., Adrover A. and Giustiniani M., (1997) *Renormalisation Analysis and Adsorption on Fractal and Disordered Lattices in the Presence of Energetic Disorder,* Langmuir, 13, pp1128-1137.

[20] Rinzel J. and Keller J.B., (1973) *Travelling Wave Solutions of Nerve Conduction Equation,* Biophysical Journal, Vol. 13, pp1313-1337.

[21] Abdulbake J., Mulholland A.J. and Gomatam J. (2003)*A Renormalisation Approach to Reaction-Diffusion Processes on Fractals*, Fractals, 11(4), pp315-330.

[22] Abdulbake J., Mulholland A.J. and Gomatam J. (2004)*Existence and Stability of Reaction-Diffusion Waves on a Fractal Lattice*, Chaos, Solitons and Fractals, 20(4), pp799-814.

[23] Quispel G.R.W. and Sahadevan R., (1993) *Lie symmetries and the integration of difference equations*, Physics Letters A, Vol. 184, pp64-70.

[24] Moritz B., Schwalm W. and Uherka D., (1998) *Finding Lie groups that reduce the order of discrete dynamical systems*, J. Phys. A: Math. Gen., Vol. 31, pp7379-7402.

[25] Elaydi S.N., (1996) *An Introduction to Difference Equations*, Springer-Verlag New York, Inc., USA.

[26] Holmgren R.A., (1994) *A First Course in Discrete Dynamical Systems*, Springer-Verlag New York, Inc. USA.

[27] Devaney R.L., (1989) *An Introduction to Chaotic Dynamical Systems, 2nd. ed.*, Addison-Wesley Publishing Company, USA.

[28] Falconer K., (1993) *Fractal Geometry, 2nd. ed.*, John Wiley and Sons, Chichester, UK.

[29] Kelley W.G. and Peterson A.C., (2001) *Difference Equations: An Introduction with Applications. 2nd. ed.*, San Diego : Harcourt/Academic Press.

Appendix. Explicit Formulae for the Renormalisation Subspace Mappings.

The mapping $\phi : (x_n, y_n) \to (x_{n+1}, y_{n+1})$ defined by equations (29) and (30) has an explicit solution given by the mapping $\psi : (a_n, t_n) \to (x_n, y_n)$

$$x_n = \frac{a_n t_n^2 - t_n^2 - 2a_n t_n + t_n - a_n}{k t_n} \tag{39}$$

$$y_n = \frac{t_n^2 - a_n t_n^2 + a_n}{k t_n} \ . \tag{40}$$

where $a_n = \sin^2(2^n \theta_0)$, $\theta_0 = \sin^{-1}(\sqrt{a_0})$ and

$$t_n = \frac{2(1 + \sum_{j=0}^{n} \frac{\prod_{i=0}^{j-1} \sec(2^{i+1}\theta_0)}{2^{j+1}})}{1 + \sum_{j=0}^{n-1} \frac{\prod_{i=0}^{j-1} \sec(2^{i+1}\theta_0)}{2^{j+1}}} - 1. \tag{41}$$

Proof

The inverse transformation ψ^{-1} is given by

$$a_n = \frac{k^2 y_n^2 - k^2 x_n^2 - 2k x_n - 1}{4k x_n} \tag{42}$$

$$t_n = \frac{k y_n - k x_n + 1}{k y_n + k x_n + 1} \ , \tag{43}$$

and the composition $\Phi = \psi^{-1} \phi \psi : (a_n, t_n) \to (a_{n+1, t_{n+1}})$ is then

$$a_{n+1} = 4a_n(1 - a_n) \tag{44}$$

$$t_{n+1} = \frac{2(a_n - t_n + a_n t_n)}{(-1 + 2a_n)(1 + t_n)} \ . \tag{45}$$

Equation (44) is the logistic equation with $\lambda = 4$, which has solution, ([28], p.195), $a_n = \sin^2(2^n\theta_0)$ with $\theta_0 = \sin^{-1}(\sqrt{a_0})$. Now let, ([25], p93)

$$\frac{z_{n+1}}{z_n} = t_n + 1 \ . \tag{46}$$

Then equation (45) gives

$$z_{n+2} + \frac{3 - 4a_n}{2a_n - 1} z_{n+1} - \frac{2}{2a_n - 1} z_n = 0 \ . \tag{47}$$

Introducing the discrete operator E, where $Ez_n = z_{n+1}$, gives ([29], p75)

$$(E + \frac{1}{2a_n - 1})(E - 2)z_n = 0 \ .$$

If $v_n = (E-2)z_n$ then $v_{n+1} = \dfrac{1}{1-2a_n} v_n$. Hence

$$(E-2)z_n = v_0 \prod_{i=0}^{n-1} (\frac{1}{1-2a_i}) = r_n \ , \qquad \text{where} \qquad \prod_{i=0}^{-1} = 1 \ . \tag{48}$$

The homogeneous part of (48) has solution $z_n^H = 2^n z_0$. Now substituting $z_n = z_n^H v_n$ into (48) gives $(E-2)z_n^H v_n = r_n$ and so $z_{n+1}^H v_{n+1} = r_n$. Hence $v_{n+1} = v_n + \dfrac{r_n}{2z_n^H}$ since $2z_n^H = z_{n+1}^H$. In general then,

$$v_n = v_0 + \sum_{j=0}^{n-1} \frac{r_j}{2z_j^H} \ ,$$

and so

$$z_n = z_n^H v_n = 2^n z_0 \left[v_0 + \sum_{j=0}^{n-1} \frac{v_0 \prod_{i=0}^{j-1} (\frac{1}{1-2a_i})}{z_0 2^{j+1}} \right] \ .$$

Since $1 - 2a_i = 1 - 2\sin^2(2^i\theta_0) = \cos(2^{i+1}\theta_0)$, where $v_0 = z_1 - 2z_0$, then, by setting $z_0 = 1$, $z_1 = t_0 + 1$, (46) becomes

$$t_n = \frac{2(1 + \sum_{j=0}^{n} \dfrac{\prod_{i=0}^{j-1} \sec(2^{i+1}\theta_0)}{2^{j+1}})}{1 + \sum_{j=0}^{n-1} \dfrac{\prod_{i=0}^{j-1} \sec(2^{i+1}\theta_0)}{2^{j+1}}} - 1 \ . \tag{49}$$